Journal of Solid State Chemistry **148,** 236–241 (1999)
Article ID jssc.1999.8442, available online at http://www.idealibrary.com on IDEAL®

The Crystallographic and Magnetoresistance of CaF_2 Doped $Nd_{0.67}Sr_{0.33}MnO_3$ Compounds

Yongquan Guo,*,†,[1] Yaocheng Liu,†,‡ Kun Tao,† Heping Zhou,† and Roger Wäplling*

*Department of Physics, Uppsala University, Box 530, S-751 21 Uppsala, Sweden; †Department of Materials Science and Engineering, Tsinghua University, Beijing 100084, People's Republic of China; and ‡State Key Laboratory of New Ceramics and Fine Processing, Beijing 100084, People's Republic of China

Received February 16, 1999; in revised form June 15, 1999; accepted July 2, 1999

We have studied crystal structures and the giant magnetoresistance of fluoride $Nd_{0.67}Sr_{0.33}MnO_3$ compounds. The experimental results show that the CaF_2 dopant can stabilize the original crystal structure of $Nd_{0.67}Sr_{0.33}MnO_3$ compounds. The lattice spacings and unit cell volumes of these fluoride compounds decrease with CaF_2 doping. The Rietveld profile fitting technique has been used to refine the crystal structures of these compounds. The space group of those compounds is *Pbnm*, $Z=4$. The F anion prefers to occupy the 8*d* crystal position. All of these fluoride compounds are ferromagnetic; their Curie temperatures decrease with CaF_2 doping. However, the giant magnetoresistance ratio of these fluoride compounds increases. A magnetoresistance ratio as high as 99.2% is obtained at an applied field of 5 *T*.

1. INTRODUCTION

The phenomenon of intrinsic giant magnetoresistance (GMR) in oxides has been known for a long time (1–3). However, recent observations of a large GMR effect in ferromagnetic metallic oxides $R_{1-x}A_xMnO_3$ (R = La, Pr, Nd, Bi; A = Ca, Sr, Ba, Pb) (4–12) have triggered renewed attention to this class of materials. A very large magnetoresistance ratio, which was very close to 100%, was reported in epitaxially grown $La_{0.67}Ca_{0.33}MnO_3$ films (13). Recently, some researches have focused on the substitution of the Mn crystal position, such as Fe, Co, Ni, and Ru elements that occupy the Mn position (15–18). Millis introduced an electron–lattice interaction model to explain the colossal magnetoresistance of managanese perovskites (19). This model is based on the electron–lattice coupling, which includes tolerance factors, the Jahn–Teller effect, double exchange interaction, and polarons. On one hand, the tolerance factors can affect the static crystal structure effect on electron hopping, which involves the conventional dynamical electron–phonon coupling. On the other hand, it can link instantaneous deviations of atoms from their ideal crystallographic positions to the instantaneous deviations of electron configuration from the average values. The Jahn–Teller model involved is derived from the distortions of the MnO_6 octahedron, which can change the e_g charge density of the Mn cation. The electronic ground state of the Mn^{3+} ions is degenerate, and its energy is lowered by a spontaneous distortion of the surrounding lattice. The double exchange interaction between Mn^{3+} and Mn^{4+} could be used to explain the GMR effect of these materials. The charge carriers are strongly coupled to the Mn cations in these materials. The local lattice distortions could also play an important role in determining the electronic and magnetic properties of these materials. In the double exchange model, the ratio of Mn^{4+} and Mn^{3+} is very important for magnetic properties and magnetic moments, as well as magnetoresistance (MR). The ratio of Mn^{4+} and Mn^{3+} can be controlled by the use of dopants with different valence states in the A, B, and O position, or by changing the oxygen content. However, up to now, there are only very limited reports on the effect of substitution of O by other elements. The effects of varying of oxygen isotope mass (O^{16} to O^{18}) have been reported by Zhao *et al.* (20). Meanwhile, the effects of changing the oxygen content in ABO_3-type perovskites (21–23) have also been studied.

In this article, we report our investigation about the crystal structures and GMR of fluoriding the $Nd_{0.67}Sr_{0.33}MnO_3$ compounds. It is found that the CaF_2 dopant does not affect the stability of original crystal structure of $Nd_{0.67}Sr_{0.33}MnO_3$. The Curie temperatures of these fluoride compounds decrease when doped with CaF_2. The GMR ratios increase significantly with CaF_2 dopants, while their GMR transition temperatures tend to decrease.

2. EXPERIMENTAL PROCEDURE

The samples of fluorine-doped $Nd_{0.67}Sr_{0.33}MnO_3$ were synthesized by a solid state reaction. The starting materials

[1] Current address: Max-Planck-Institute for Chemical Physics of Solids, Pirnaer Landstr. 176, Gebaude 324, 01257 Dresden, Germany.

0022-4596/99 $30.00

Nd_2O_3, MnO_2, $SrCO_3$, and 2–20 mol% CaF_2 were mixed in stoichiometeric proportions and were calcined at 1273 K for 20 h. The powder thus obtained was ground, palletized, and sintered at 1473 K for 40 h with two intermediate grindings, then cooled to room temperature. The X-ray diffraction (XRD) intensity data, which were used for crystal structure analysis, were collected by a Rigaku automatic diffractometer with a rotating anode and a 12 kW X-ray generator. Cu$K\alpha_1$ radiation ($\lambda = 1.5406$ Å) and a graphic monochrometer for diffracted beams were used. A step scanning mode was adopted, with a scanning step of 0.02° (2θ). The positions of diffraction peaks were corrected by using high purity Si as an internal standard. After normalization, the TREOR program (24) was used in indexing the XRD patterns. The diffraction data were analyzed by using Rietveld's powder diffraction profile-fitting technique (25) to determine the crystal structural parameters. The thermomagnetic properties and magnetoresistance of these samples were determined by sample magnetometer measurements from 1.5 K to room temperature, with an applied field of 500 Oe. The magnetoresistance was measured at zero field and 5 T, respectively.

3. EXPERIMENTAL RESULTS AND DISCUSSION

The powder XRD exhibits the single phase orthogonally distorted perovskite structure for all samples after two heat treatments. The space group of orthorhombic structure is *Pbnm*, with $Z = 4$. The refined lattice parameters of these compounds are $a = 5.433(0)$–$5.465(6)$ Å, $b = 5.451(3)$–$5.454(9)$ Å and $c = 7.671(3)$–$7.697(7)$ Å. The lattice parameters and unit cell volumes of these compounds decrease with CaF_2 dopant. The reason might be that the radii of Ca^{2+} and F^- ions are less than those of (Sr^{2+}, Nd^{3+}) and O^{2-}, respectively. The variation of lattice parameter and unit cell volume vs CaF_2 content is given in Fig. 1. These results indicate that the substitution of O by F still could stabilize the original crystal structure. The crystal structures of all samples are refined by Rietveld's profile-fitting technique. The refined XRD pattern of the sample with 20 mol% CaF_2 is taken as a typical example, and the experimental and calculated XRD patterns of this sample are displayed in Fig. 2. In this figure, the experimental and calculated patterns are marked by " + " and a solid line, respectively. The lowest trace indicates the difference between the calculated and the experimental patterns, and the peak positions of the orthorhombic structure are marked by the middle vertical lines. The residual factor is $R_p = 9.60\%$, the weighted residual factor is $R_{wp} = 11.91\%$, and the goodness of fit factor is $s = 1.80$. Table 1 shows the refined structural parameters and ionic positions for all samples. The nearest neighbor bond lengths of the Mn ions and the bond angles of the strong Mn–O bond are listed in Table 2.

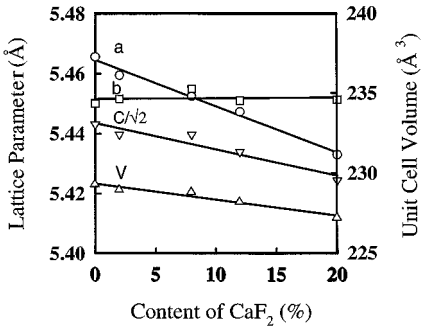

FIG. 1. The variation of lattice parameter and unit cell volume vs CaF_2 content.

The temperature dependence of the magnetization of all of samples is measured at an applied field of 500 Oe; the results are given in Fig. 3. All of these compounds are ferromagnetic; their Curie temperatures decrease by CaF_2 doping. The magnetoresistance of these compounds was measured at zero field and an applied field of 5 T from 1.5 K to room temperature. The temperature dependence of the MR and MR ratio are given in Figs. 4a, 4b, and 5, respectively. The MR ratios are defined as $[R(0) - R(H)]/R(H = 0)$, where $R(0)$ and $R(H)$ correspond to the resistance at zero and applied magnetic fields. The largest MR ratio appears in the sample with 20% CaF_2 doping, with a value of 99.2%. Others exhibit values greater than 70.5%. Table 3 gives the experimental data of T_C, T_m, and the MR ratios. The experimental results show that the MR ratios of samples increase with rising CaF_2 content. However, the magnetoresistance transition temperatures of these compounds decrease from 211.9 to 124.2 K. The gap between the Curie temperature T_C and the magnetoresistance transition temperature T_m tends to increase. According to recent reports (26, 27), with a decrease in the average ionic radius of the La

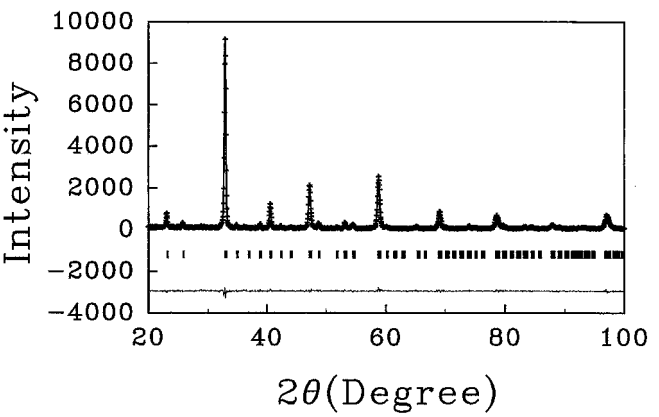

FIG. 2. The experimental and calculated XRD pattern of sample with 20 mol% CaF_2 doping.

TABLE 1
The Refined Structural Parameters, Numbers of Ions, and Ionic Occupations of Fluoride $Nd_{0.67}Sr_{0.33}MnO_3$ Compounds

Ionic occupations	No dopant	2 mol% CaF_2	8 mol% CaF_2	12 mol% CaF_2	20 mol% CaF_2
Space group	*Pbnm*	*Pbnm*	*Pbnm*	*Pbnm*	*Pbnm*
Z	4	4	4	4	4
a (Å)	5.465(6)	5.459(5)	5.452(5)	5.447(3)	5.433(0)
b (Å)	5.450(1)	5.451(6)	5.454(9)	5.451(0)	5.451(3)
c (Å)	7.697(7)	7.695(4)	7.692(9)	7.684(7)	7.671(3)
v (Å^3)	229.3(0)	229.0(3)	228.8(1)	228.1(8)	227.2(0)
4*a* Mn^{4+}/Mn^{3+}	*x*, 0	0	0	0	0
	y, 0	0	0	0	0
	z, 0	0	0	0	0
Numbers of Mn	4,	4,	4, 0,	4	4
4*c* R(Nd^{3+}, Sr^{2+}, Ca^{2+})	*x*, 0.4940(1)	0.4935(9)	0.4944(2)	0.4948(4)	0.4975(5)
	y, 0.0224(6)	0.0241(2)	0.0254(1)	0.0269(3)	0.0302(0)
	z, 0.25	0.25	0.25	0.25	0.25
Numbers of Nd	2.67	2.61	2.45	2.35	2.21
Numbers of Sr	1.33	1.31	1.23	1.18	1.07
Numbers of Ca	0	0.08	0.32	0.47	0.80
4*c* O^{2-} (I)	*x*, 0.5567(4)	0.5371(8)	0.5420(5)	0.5869(5)	0.5713(3)
	y, 0.4968(5)	0.5031(3)	0.5004(4)	0.4905(4)	0.4945(3)
	z, 0.25	0.25	0.25	0.25	0.25
Numbers of O(I)	4	4	4	4	4
8*d* O(O^{2-}(II), F^-)	*x*, 0.2127(3)	0.2105(8)	0.2120(1)	0.2153(2)	0.2154(4)
	y, 0.2536(4)	0.2502(6)	0.2509(2)	0.2666(7)	0.2779(4)
	z, 0.0266(7)	0.0261(1)	0.0361(8)	0.0249(0)	0.0367(4)
Numbers of O(II)	8	7.81	7.40	6.98	6.11
Numbers of F	0	0.14	0.61	0.90	1.42
R_p	9.7%	10.3%	12%	9.6%	9.6%
R_{wp}	12·6%	13.7%	15.6%	12.8%	11.9%
s	1.9	2.0	2.2	1.8	1.8

site $\langle r \rangle$, T_C decreases; however, the MR ratio increases. Under our experimental conditions, the lattice spacings of fluoride (Nd, Sr)MnO_3 compounds decrease and the average ionic radius of the La site $\langle r \rangle$ also decreases. Thus, the experimental results are the same as those reported before (26, 27); that is, the Curie temperature decreases and the MR ratio rises. Meanwhile, magnetic order and significant magnetoresistance effects are noted at low temperature. The reason for this phenomenon is that the notion of double exchange must be generalized to include changes in the Mn–O–Mn electronic hopping parameters as a result of changes in the Mn–O–Mn bond angle (28).

The geometry of the Mn–O–Mn bond plays a crucial role since the O anion mediates the double exchange. In a stoichiometric perovskite structure, the Mn cations occupy the center of the oxygen octahedra, with a 180° bond angle. The distortion of the crystal structure results in a buckling of the octahedral network. Thus the change of the Mn–O–Mn bond angle and bond lengths can affect the electron hopping probability and the double-exchange interaction. In our experiment, the effect of CaF_2 dopant in the Mn–O–Mn bond lengths and bond angles is significant. The Mn–(O (II), F) bond lengths increase with CaF_2 doping. Of the inequivalent Mn–(O(II), F) bonds, one decreases and

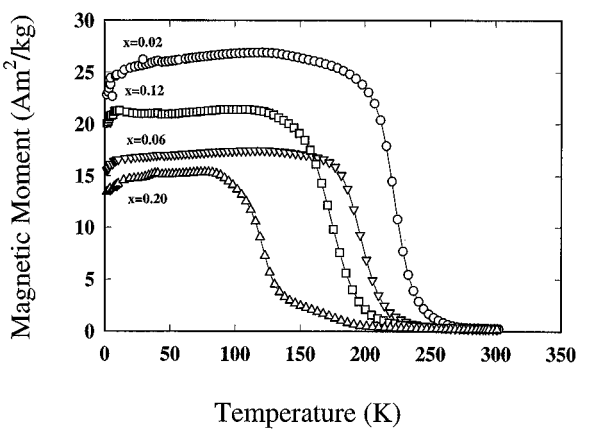

FIG. 3. The temperature dependence of magnetization of fluoride $Nd_{0.67}Sr_{0.33}MnO_3$ compounds. *x* denotes the content of CaF_2 dopant.

TABLE 2
Bond Lengths (BL) and Nearest Neighbors (NN) of Fluoride $Nd_{0.67}Ca_{0.33}MnO_3$ Compounds

Ion Ion	No dopant (BL(Å) and NN)	2 mol% CaF_2 (BL(Å) and NN)	8 mol% CaF_2 (BL(Å) and NN)	12 mol% CaF_2 (BL(Å) and NN)	20 mol% CaF_2 (BL(Å) and NN)
Mn–2O(I)	1.949	1.935	1.937	1.979	1.957
–2(O (II), F)	1.818 6	1.795 6	1.838 6	1.878 6	1.935 6
–2(O (II), F)	2.076	2.095	2.074	2.015	1.984
⟨Mn–O⟩	1.948	1.942	1.950	1.957	1.959
O(I)–2(O (II), F)	2.661	2.572	2.566	2.630	2.734
–2(O (II), F)	2.670	2.705	2.771	2.716	2.678
–2(O (II), *F*)	2.824	2.837	2.776	2.823	2.778
–2(O (II), F)	2.872	2.867	2.898	2.929	2.794
–1(Nd, Sr, Ca)	2.459 14	2.564 14	2.531 14	2.387 14	2.350 14
–1(Nd, Sr, Ca)	2.608	2.622	2.604	2.576	2.563
–1(Nd, Sr, Ca)	2.885	2.850	2.875	2.967	2.947
–1(Nd, Sr, Ca)	3.013	2.900	2.928	3.175	3.097
–2Mn	1.949	1.935	1.937	1.979	1.957
O(II), F–2(O (II), F)	2.755	2.759	2.759	2.750	2.751
–2(O (II), F)	2.764	2.760	2.784	2.756	2.791
–1O (I)	2.661	2.572	2.566	2.630	2.734
–1O(I)	2.670	2.705	2.771	2.716	2.767
–1O(I)	2.824 14	2.837 14	2.776 14	2.823 14	2.778 14
–1O (I)	2.872	2.867	2.898	2.929	2.794
–1Mn	1.818	1.795	1.838	1.878	1.935
–1Mn	2.076	2.095	2.074	2.015	1.984
–1(Nd, Sr, Ca)	2.526	2.564	2.473	2.513	2.430
–1(Nd, Sr, Ca)	2.628	2.622	2.583	2.649	2.617
–1(Nd, Sr, Ca)	2.730	2.850	2.768	2.678	2.708
–1(Nd, Sr, Ca)	3.061	2.900	3.127	3.085	3.177
Nd, Sr, Ca–1O(I)	2.459	2.564	2.531	2.387	2.350
–1O(I)	2.608	2.622	2.604	2.576	2.563
–1O(I)	2.885	2.850	2.875	2.967	2.947
–1O(I)	3.013 8	2.900 8	2.928 8	3.175 8	3.097 14
–1O(II)	2.526	2.538	2.473	2.513	2.430
–IO(II)	2.628	2.622	2.583	2.649	2.617
–IO(II)	2.730	2.726	2.768	2.678	2.708
–1O (II)	3.061	3.060	3.127	3.085	3.177
O (I)–Mn–O(I) bond angle	180°	180°	180°	177.36°	180°
O (III)–Mn–O (II) bond angle	89.81°	89.75°	89.49°	89.90°	89.16

the another one increases. The average Mn–O bond length increases from 1.948 to 1.959 Å; this may be the reason for the declining T_C. On other hand, changes in bond length and angle might result in the formation of a Jahn–Teller polaron and thereby affects the MR ratio.

Xiong *et al.* had studied the GMR effects of epitaxial $Nd_{0.7}Sr_{0.3}MnO_{3-\delta}$ thin films (10). According to their report, the MR ratio was close to 97% under an applied field (5*T*), and the magnetoresistance transition temperature occurred at 95 K. However, we have obtained the largest MR ratio of 99.2% by F doping under the same experimental condition; in our work the magnetoresistance transition occurred at 124.2 K. This implies that F can affect magnetic properties and magnetoresistance of the original compound. According to our refind results, the occupation rates for Ca cations in the A position increase with the CaF_2 dopant; thus the Mn^{4+}/Mn^{3+} ratio rises. However, the substitution ratio for F to O could not always be kept at 2 to 1 under our heat treatment condition. Thus, F^- substitution for O^{2-} could increase the Mn^{3+} content and hereby decrease the Mn^{4+}/Mn^{3+} ratio. This implies that there is a competition between F anion and Ca cation doping. This competition affects the Mn^{4+}/Mn^{3+} ratio and thereby affects the magnetic properties and GMR effect of these compounds.

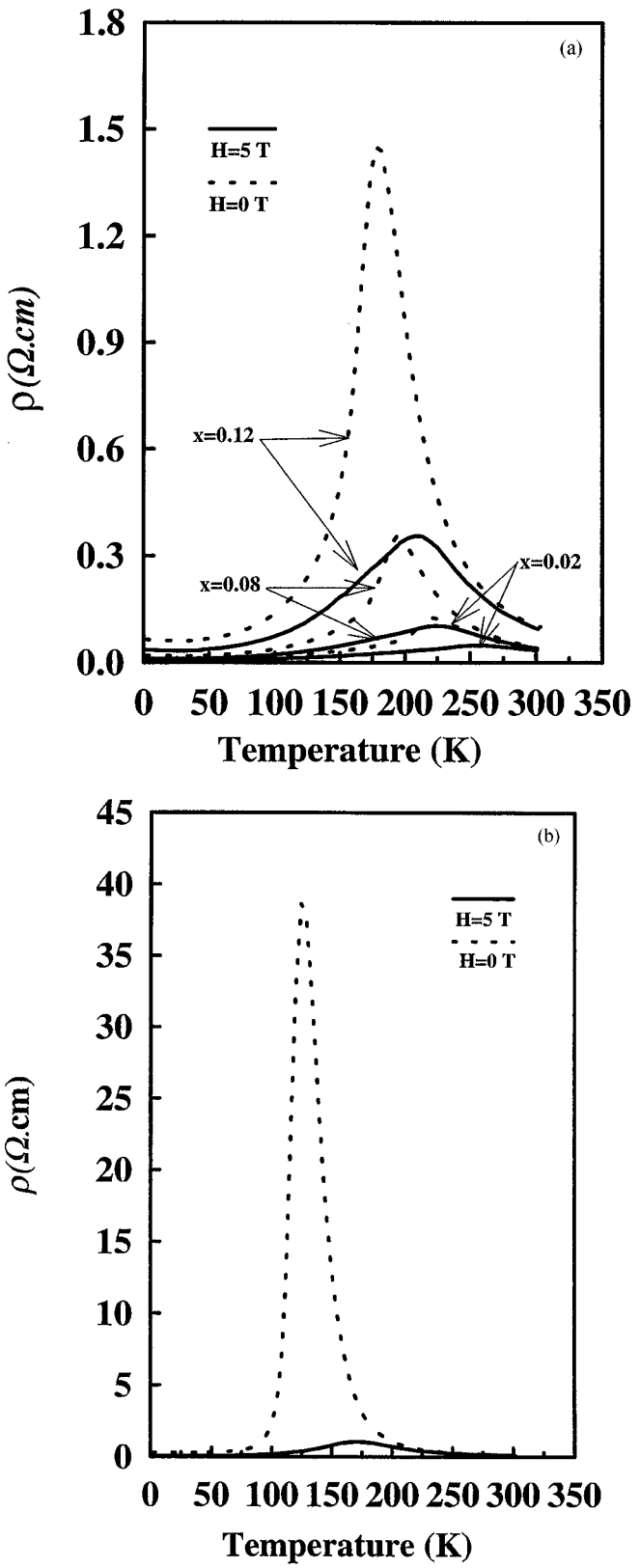

FIG. 4. The temperature dependence of the magnetoresistance of fluoride $Nd_{0.67}Sr_{0.33}MnO_3$ compounds. (a) and (b) correspond to those samples with 2–12 mol% and 20 mol % CaF_2 dopant.

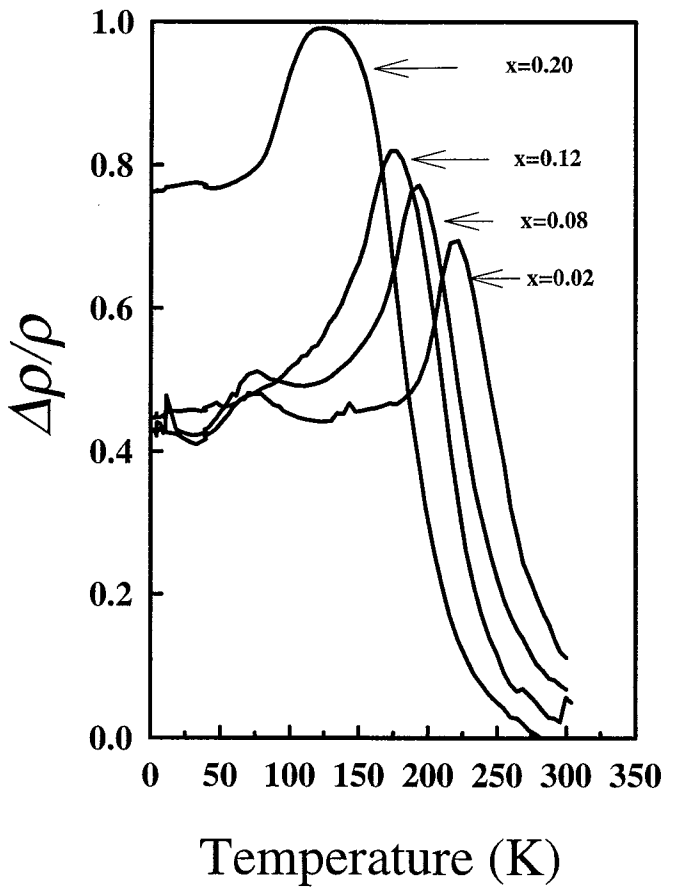

FIG. 5. The temperature dependence of MR ratios of all samples.

4. CONCLUSION

We have studied the crystal structures and giant magnetoresistance of fluoride $Nd_{0.67}Sr_{0.33}MnO_3$ compounds. The lattice parameters and until cell volumes of these compounds decrease with the CaF_2 doping. The space group is *Pbnm*, with $Z = 4$. The CaF_2 dopant does not affect the stability of the original crystal structure of $Nd_{0.67}Sr_{0.33}MnO_3$. The refined results indicate that the F anion prefers to occupy the 8*d* crystal position. The Curie

TABLE 3
Curie Temperatures (T_C), Magnetoresistance Transition Tempertures (T_m), and MR Ratios for all Samples

CaF_2 content (mol %)	T_C (K)	T_m (K)	MR ratio (%)
2	252.4	211.9	70.5
8	219.1	193.5	77.2
12	204.9	177.0	81.2
20	172.2	124.2	99.2

temperatures of these fluoride compounds decrease with CaF_2 doping; however, their GMR ratios increase significantly with CaF_2 doping, and their GMR transition temperatures tend to decrease. The largest MR ratio is 99.2%.

REFERENCES

1. E. Pytte, *Phys. Rev. B* **10,** 4637 (1974).
2. E. O. Wollan and W. F. Koehler, *Phys. Rev.* **100,** 545 (1955).
3. L. N. Bulaevski, *Sov. Phys. Solid State* **11,** 921 (1969).
4. C. W. Searle and S. T. Wang, *Can. J. Phys.* **48,** 2023 (1970).
5. G. M. Jonker and J. H. van Santen, *Physica* **16,** 337 (1950).
6. S. Huizinga *et al*., *Phys. Rev. B* **19,** 4723 (1979).
7. C. Coulon *et al*., *Synth. Met*. **27,** *B*449 (1988).
8. H. Kawano *et al*., *Phys. Rev. B* **53,** R14709 (1996).
9. M. Hase *et al*., *Phys. Rev. Lett*. **70,** 3651 (1993).
10. G. C. Xiong *et al*., *Appl. Phys. Lett*. **66,** 1427 (1995).
11. R. von Helmolt *et al*., *Phys. Rev. Lett*. **71,** 2331 (1993).
12. S. Jin *et al*., *Science* **264,** 413 (1994).
13. W. Bao *et al*., *Phys. Rev. Lett*. **78,** 543 (1997).
14. K. Chahara *et al*., *Appl. Phys. Lett*. **63,** 1990 (1993).
15. K. H. Ahn *et al*., *Phys. Rev. B* **54,** 15299 (1997).
16. G. Briceno, *Science* **270,** 273 (1995).
17. M. Z. Medarde, *J. Phys. Conden. Mater* **9,** 1679 (1997).
18. G. Cao, S. Mccall, and J. E. Crow, *Phys. Rev. Lett*. **78,** 1751 (1997).
19. A. J. Millis, *Nature* **392,** 147 (1998).
20. G. M. Zhao *et al*., *Nature* **381,** 676 (1996).
21. H. L. Ju *et al. Phys. Rev*., *B* **51,** 6143 (1995).
22. X. X. Zhang *et al*., *Appl. Phys. Lett*. **63,** 3191 (1996).
23. H. L. Ju *et al*., *Appl. Phys. Lett*. **65,** 2108 (1994).
24. P. E. Winner, *J. Appl. Cryst*. **9,** 594 (1965).
25. H. M. Rietveld, *J. Appl. Cryst*. **2,** 65 (1969).
26. Z. B. Guo, *Solid State Commun*. **100,** 769 (1996).
27. H. Y. Hwang *et al*., *Phys. Rev. Lett*. **75,** 914 (1995).
28. K. Liu *et al*., *Phys. Rev*. **54,** 3007 (1996).